A probability density function/flamelet method for partially premixed turbulent combustion

By D. C. Haworth†

A methodology is formulated to accommodate detailed chemical kinetics, realistic turbulence/chemistry interaction, and partially premixed reactants in three-dimensional time-dependent device-scale computations. Specifically, probability density function (PDF) methods are combined with premixed laminar flamelet models to simulate combustion in stratified-charge spark-ignition reciprocating-piston IC engines. A hybrid Lagrangian/Eulerian solution strategy is implemented in an unstructured deforming-mesh engineering CFD code. Modeling issues are discussed in the context of a canonical problem: one-dimensional constant-volume premixed turbulent flame propagation. Three-dimensional time-dependent demonstration calculations are presented for a simple pancake-chamber engine.

1. Introduction

In most practical combustion devices, the conversion of chemical energy to sensible energy takes place in a turbulent flow environment. A variety of turbulent combustion models have been implemented in computational fluid dynamics (CFD) codes to facilitate device-scale analysis and design. In general, a different modeling approach has been required to deal with each combustion regime (e.g., premixed versus nonpremixed). Next-generation low-emission/low-fuel-consumption combustion systems are characterized by multiple combustion regimes, i.e., "mixed-mode" or "partially premixed" turbulent combustion. Examples include lean premixed combustion systems for reducing NO_X emissions from gas-turbine combustors and gasoline direct-injection spark-ignition engines for reducing the fuel consumption of personal transportation vehicles (Zhao, Lai & Harrington 1999).

Next-generation turbulent combustion models for device-scale CFD also must include detailed chemical kinetics and must be suitable for three-dimensional time-dependent calculations (e.g., large-eddy simulation - LES) in complex geometric configurations. More chemistry is required to deal with kinetically controlled phenomena (e.g., low-temperature autoignition) to predict trace pollutant species (e.g., NO_x, unburned hydrocarbons, particulate matter) and to address fuel-composition issues (e.g., alternative fuels and fuel additives). Increasingly, the phenomena of interest are inherently three-dimensional and time-dependent. For example, it is unlikely that statistically stationary computations will suffice to address combustion instabilities in gas-turbine combustors. And the ensemble-averaged formulation that has been dominant in piston-engine modeling (e.g., Khalighi *et al.* 1995) cannot capture cycle-to-cycle flow and combustion variability.

Thus an outstanding modeling/methodology issue in turbulent combustion can be

† The Pennsylvania State University

stated as: how can increasingly complex chemical kinetics, realistic turbulence/chemistry interaction, and multiple combustion regimes be accommodated in three-dimensional time-dependent device-scale CFD? It is the purpose of this report to formulate, implement, and provide an initial demonstration of an approach that addresses this question.

The model is a hybrid of two of the most promising approaches for turbulent reacting flows: probability density function (PDF) methods and laminar flamelet models. PDF methods have the important advantage that the mean chemical source term appears in closed form; molecular transport ("mixing") remains to be modeled (Pope 1985). While advantages of PDF methods have been amply demonstrated in laboratory configurations, device-scale application has been slowed by the unconventional Lagrangian particle-based algorithms that are used to solve PDF transport equations numerically. Flamelet models, on the other hand, maintain strong coupling between chemical reaction and molecular transport (Peters 2000). However, the coupling is correct only under specific (essentially boundary-layer-like) conditions, which are not always valid in practical combustion devices. In cases where flamelet combustion does occur (e.g., homogeneous flame propagation in a stoichiometric premixed spark-ignition engine), flamelet models have proven highly successful. It is relatively straightforward to implement flamelet models in standard Eulerian grid-based CFD codes.

Following earlier work on PDF methods for complex geometric configurations, a hybrid Lagrangian/Eulerian strategy is adopted. Several implementation issues including mean estimation, particle tracking through unstructured deforming meshes, and particle number density control have been addressed by Subramaniam & Haworth (2000). There a composition PDF method and Reynolds-averaged (RANS) formulation were used to model turbulent mixing with large density variation in an engine-like configuration. Other key issues in Lagrangian/Eulerian PDF methods have been addressed by Muradoglu *et al.* (1999).

The present report expands on Subramaniam & Haworth (2000) in several respects. First, heat release is included. Second, a hybrid PDF/flamelet method is formulated to take advantage of the strengths of each these two modeling approaches. Third, both velocity-composition PDF and composition PDF methods are explored. Fourth, physical and numerical issues are discussed in the context of a canonical problem (turbulent premixed flame propagation in a one-dimensional constant-volume chamber). And finally, preliminary three-dimensional time-dependent RANS computations are presented for a simple piston-engine configuration.

2. Formulation

The approach is developed in the context of a stratified-charge gasoline-direct-injection spark-ignition piston engine. A three-stage combustion process is postulated (Fig. 1). By design, a healthy propagating premixed flame is established initially via spark discharge at a location where the composition is close to stoichiometric. Soon (within a few millimeters, depending on engine operating conditions), the flame encounters fuel-rich and fuel-lean mixtures. Behind the flame in locally fuel-rich zones are combustion products and fuel fragments (mainly the stable intermediates CO and H_2, to be precise); behind the flame in locally fuel-lean zones are combustion products and oxygen. Eventually the post-flame fuel fragments and oxygen combine to complete the heat-release process. Stage I aerothermochemical processes (in front of the primary flame) include turbulent mixing and low-temperature chemistry (e.g., autoignition, under suitable operating con-

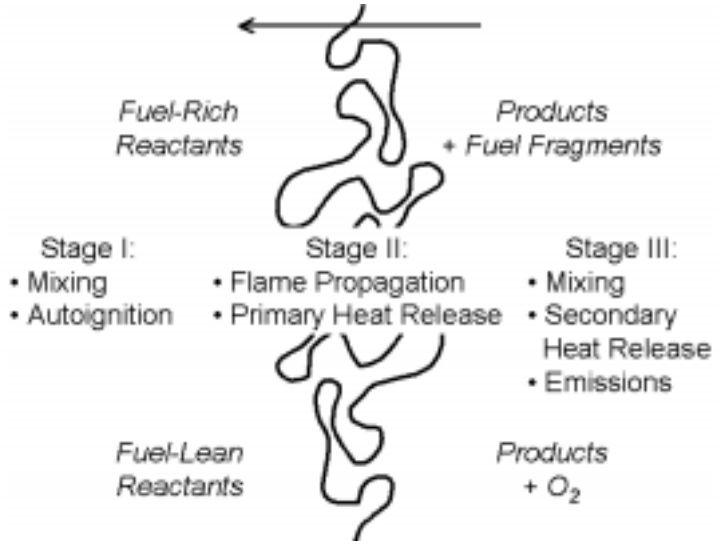

FIGURE 1. A three-stage combustion process for partially premixed reactants.

ditions). Stage II comprises flame propagation and the primary heat release. And Stage III (behind the primary flame) includes turbulent mixing, secondary heat release, and the finite-rate chemistry that characterizes key pollutant-formation processes such as CO burnout, NO_x formation, and soot formation/oxidation.

Finite-rate chemistry and turbulence/chemistry interaction in Stages I and III are naturally described using a PDF formulation, while the flame propagation of Stage II is amenable to laminar flamelet modeling. The essence of the approach is to combine these two models in a consistent manner that deals naturally with all three regimes.

2.1. *Governing equations*

Reynolds-averaged equations are used in density-weighted (Favre-averaged) form. Thus the PDF's considered formally are mass-density functions (Pope 1985). A multicomponent reacting ideal-gas mixture comprising N_S chemical species is considered. At low Mach number, the mixture mass density ρ and chemical production rates $\underline{S}$ are functions of species mass fractions $\underline{Y}$, enthalpy h, and a reference pressure p_0 that is, at most, a function of time: $\rho = \rho\big(\underline{Y}, h, p_0(t)\big)$, $\underline{S} = \underline{S}\big(\underline{Y}, h, p_0(t)\big)$. Key Eulerian equations express conservation of mixture mass, momentum, enthalpy, and species mass. A conventional two-equation $\widetilde{k} - \widetilde{\epsilon}$ turbulence model with wall functions is invoked (e.g., Khalighi *et al.* 1995). The mean momentum and enthalpy equations have the form:

$$\frac{\partial[\langle\rho\rangle\widetilde{u}_i]}{\partial t} + \frac{\partial[\langle\rho\rangle\widetilde{u}_j\widetilde{u}_i]}{\partial x_j} = -\frac{\partial\langle p\rangle}{\partial x_i} + \frac{\partial(\langle\tau_{ji}\rangle + \tau_{T,ji})}{\partial x_j} \quad , \tag{2.1}$$

$$\begin{aligned}\frac{\partial[\langle\rho\rangle\widetilde{h}]}{\partial t} + \frac{\partial[\langle\rho\rangle\widetilde{u}_j\widetilde{h}]}{\partial x_j} &= \frac{\partial\langle p\rangle}{\partial t} + \widetilde{u}_j\frac{\partial\langle p\rangle}{\partial x_j} + \mu\Big(\frac{\partial\widetilde{u}_i}{\partial x_j} + \frac{\partial\widetilde{u}_j}{\partial x_i}\Big)\frac{\partial\widetilde{u}_i}{\partial x_j} + \langle\rho\rangle\widetilde{\epsilon} \\ &\quad - \frac{2}{3}\mu\frac{\partial\widetilde{u}_i}{\partial x_i}\frac{\partial\widetilde{u}_j}{\partial x_j} + \frac{\partial}{\partial x_j}\Big[\Big(\frac{\lambda}{C_p} + \frac{\mu_T}{\sigma_{T,h}}\Big)\frac{\partial\widetilde{h}}{\partial x_j}\Big] \quad .\end{aligned} \tag{2.2}$$

Here $\underline{u}$ denotes velocity, p pressure, and h enthalpy: $h \equiv \sum_{\alpha=1}^{N_S} Y_\alpha \big(\Delta h^0_{f,\alpha} + \int_{T^0}^{T} C_{p,\alpha}(T')dT'\big)$, $\Delta h^0_{f,\alpha}$ being the species-α formation enthalpy at reference temperature T^0. The viscous stress is $\tau_{ji} = \mu(\partial u_j/\partial x_i + \partial u_i/\partial x_j) - \frac{2}{3}\mu\partial u_l/\partial x_l \delta_{ji}$. A tilde $\widetilde{\ }$ denotes a Favre-averaged mean quantity, while angled brackets $\langle\ \rangle$ are used for the conventional mean; a double-prime denotes a fluctuation about the Favre mean. Mixture molecular transport coefficients are the viscosity μ and thermal conductivity λ; C_p is the mixture specific heat (at constant pressure). The effective turbulent stress is $\tau_{T,ji} = -\langle\rho\rangle\widetilde{u''_j u''_i} = \mu_T(\partial\widetilde{u}_j/\partial x_i + \partial\widetilde{u}_i/\partial x_j) - \frac{2}{3}\mu_T\partial\widetilde{u}_l/\partial x_l\delta_{ji} - \frac{2}{3}\langle\rho\rangle\widetilde{k}\delta_{ji}$ where $\mu_T = C_\mu\langle\rho\rangle\widetilde{k}^2/\widetilde{\epsilon}$ is the effective turbulence viscosity and C_μ is a standard $\widetilde{k}-\widetilde{\epsilon}$ model constant. The turbulent Prandtl number is $\sigma_{T,h}$.

A modeled PDF transport equation governs the mixture's thermochemical state. This equation is solved using a Lagrangian method for a large number N_P of notional particles. In the case of a composition PDF, the position and composition of the i^{th} particle $(i = 1, \ldots, N_P)$ evolve by,

$$\begin{aligned} \underline{x}^{(i)}(t+\Delta t) &= \underline{x}^{(i)}(t) + \widetilde{\underline{u}}(\underline{x}^{(i)}(t), t)\Delta t + \Delta\underline{x}^{(i)}_{turb} \quad , \\ \underline{\Phi}^{(i)}(t+\Delta t) &= \underline{\Phi}^{(i)}(t) + \underline{S}^{(i)}(\underline{\Phi}^{(i)}(t), p_0(t))\Delta t + \Delta\underline{\Phi}^{(i)}_{mix} \quad . \end{aligned} \tag{2.3}$$

Here $\underline{\Phi}^{(i)}(t)$ denotes the vector of composition variables required to specify the thermochemical state of the mixture (e.g., mass fractions and enthalpy), $\Delta\underline{x}^{(i)}_{turb}$ is the increment in particle position due to turbulent diffusion in time interval Δt, and $\Delta\underline{\Phi}^{(i)}_{mix}$ is the increment in particle composition due to molecular mixing.

The above equations are supplemented by a thermal equation of state $\rho = \rho\big(\underline{Y}, T, p_0(t)\big)$, a caloric equation of state $T = T\big(\underline{Y}, h, p_0(t)\big)$, fluid property specification (molecular transport coefficients and specific heats), and a chemical reaction mechanism $\underline{S} = \underline{S}\big(\underline{Y}, h, p_0(t)\big)$. Additional equations are introduced in Section 2.3.

2.2. *Solution algorithm*

The CFD code solves the Reynolds- (Favre-) averaged compressible equations for a multicomponent reacting ideal-gas mixture using a finite-volume method on an unstructured deforming mesh of (primarily) hexahedral volume elements. Collocated cell-centered variables are used with a segregated time-implicit pressure-based algorithm similar to SIMPLE or PISO. The discretization is first-order in time and up to second-order in space. Further information can be found in Subramaniam & Haworth (2000).

2.3. *Physical models*

A hierarchy of models is considered. This staged development is intended to elucidate key aspects of the approach.

2.3.1. *Model 1*

Model 1 comprises infinitely fast chemistry, constant specific heats and molecular transport coefficients, and a composition PDF for a single scalar reaction progress variable c that ranges from zero in unburned reactants to unity in burned products (perfectly premixed reactants). Heat release is specified via a parameter which corresponds to the normalized temperature rise across an adiabatic flame: $\beta \equiv -\Delta h^0_f/(C_p T_{ref})$. Temperature and density then are simple functions of c: $T = h/C_p + c\beta T_{ref}$; $\rho = p/RT$ $(R = C_p - C_v)$.

Turbulent diffusion is modeled as a diffusion process in physical space,

$$\Delta \underline{x}^{(i)}_{turb} = [\nabla \Gamma_{T,c}/\langle\rho\rangle]_{\underline{x}^{(i)}(t)} \Delta t + [2\Delta t \Gamma_{T,c}/\langle\rho\rangle]^{1/2}_{\underline{x}^{(i)}(t)} \underline{\eta} \quad . \tag{2.4}$$

Here $\Gamma_{T,c} = C_\mu \langle\rho\rangle \sigma^{-1}_{T,c} \widetilde{k}^2/\widetilde{\epsilon}$ is a turbulent diffusivity and $\underline{\eta}$ is a vector of independent identically distributed standardized (zero mean, unit variance) Gaussian random variables.

In a laminar flamelet, chemical reaction and molecular transport are, in principle, treated exactly: $\Delta c^{(i)} = [S + \rho^{-1} \partial(\Gamma \partial c/\partial x_j)/\partial x_j]_{c^{(i)}(t)} \Delta t$. That is, both are known from the given laminar flame profile. At high Damköhler number, however, direct implementation is impractical. The length and time scales associated with the flamelet are much smaller than those associated with the PDF evolution; the latter correspond to the turbulence integral scales. Instead, following Anand & Pope (1987) the fast-chemistry limit is treated as:

$$c^{(i)}(t + \Delta t) = c^{(i)}(t) + \Delta c^{(i)}_{reaction} + \Delta c^{(i)}_{mix} \quad . \tag{2.5}$$

Here $\Delta c^{(i)}_{reaction}$ takes $c^{(i)}$ to unity as soon as $c^{(i)}$ exceeds c_{thresh} (a small positive number, of the order of the reciprocal of the Damköhler number); and $\Delta c^{(i)}_{mix}$ denotes a conventional turbulence mixing model. Here a stochastic pair-exchange model is used (Pope 1985).

Thus for Model 1, Eqs. (2.1) and (2.2) plus modeled equations for $\widetilde{k}$ and $\widetilde{\epsilon}$ are solved by a finite-volume method, and the PDF of the reaction progress variable c is computed using a stochastic particle method (Eqs. 2.3-2.5). Mean velocity and turbulence scales are passed from the finite-volume side to the particle side; and the mean density $\langle\rho\rangle$ (computed using the mean-estimation algorithm described in Subramaniam & Haworth 2000) is passed from the particle side to the finite-volume side.

2.3.2. *Model 2*

Model 2 retains the thermochemistry of Model 1 and replaces the composition PDF with a velocity-composition PDF. In this case, a finite-volume $\widetilde{k}$ equation is not needed; the turbulent stress in Eq. (2.1) and the turbulence kinetic energy $\widetilde{k}$ are computed as,

$$\tau_{T,ji} = -\langle\rho\rangle \widetilde{u''_j u''_i} \quad , \quad \widetilde{k} = (\widetilde{u''_1 u''_1} + \widetilde{u''_2 u''_2} + \widetilde{u''_3 u''_3})/2 \quad , \tag{2.6}$$

where $\widetilde{u''_j u''_i}$ is computed from particle velocities. A standard $\widetilde{\epsilon}$ equation provides the necessary turbulence scales.

The PDF transport equation is modeled and solved by considering the positions, compositions (progress variable c), and velocities of N_P notional particles. Particle progress variable is governed by Eq. (2.5) while particle positions and velocities evolve according to,

$$\begin{aligned} \underline{x}^{(i)}(t + \Delta t) &= \underline{x}^{(i)}(t) + \underline{u}^{(i)}(t) \Delta t \quad , \\ \underline{u}^{(i)}(t + \Delta t) &= \underline{u}^{(i)}(t) - \rho^{(i)\,-1} \nabla \langle p \rangle \Delta t + \Delta \underline{u}^{(i)}_{turb} \quad . \end{aligned} \tag{2.7}$$

The particle turbulent velocity increment $\Delta \underline{u}^{(i)}_{turb}$ is modeled using a simplified Langevin equation (Haworth & Pope 1987),

$$\Delta \underline{u}^{(i)}_{turb} = -(\frac{1}{2} + \frac{3}{4} C_0)(\underline{u}^{(i)} - \widetilde{\underline{u}}) \Delta t \, \widetilde{\epsilon}/\widetilde{k} + [C_0 \widetilde{\epsilon} \Delta t]^{1/2}_{\underline{x}^{(i)}(t)} \underline{\eta} \quad , \tag{2.8}$$

with the model constant $C_0 = 2.1$.

Model 2 is intentionally similar to the model developed by Anand & Pope (1987) for steady one-dimensional constant-enthalpy freely propagating turbulent premixed flames. An important difference is in the solution strategy. There a Lagrangian method limited to the problem considered (steady, one-dimensional, constant-enthalpy, unconfined flame propagation) was used; here a general-purpose three-dimensional time-dependent hybrid algorithm is adopted.

In this case Eqs. (2.1), (2.2), and a dissipation equation are solved on the finite-volume side, while Eqs. (2.5), (2.7), and (2.8) are solved on the particle side. Mean momentum effectively is computed twice: this redundancy is resolved by forcing particle mean velocities to remain consistent with the finite-volume mean. Quantities passed from the finite-volume side are the mean velocity and dissipation rate; the mean density and Reynolds stresses (Eq. 2.6) are passed from the particle side to the finite-volume side.

2.3.3. *Model 3*

In Model 3, flame propagation and primary heat release (Stage II, Fig. 1) are governed by a modeled Eulerian mean-progress-variable equation:

$$\frac{\partial[\langle\rho\rangle\widetilde{c}]}{\partial t}+\frac{\partial[\langle\rho\rangle\widetilde{u}_j\widetilde{c}]}{\partial x_j}=\frac{\partial}{\partial x_j}\Big[\big(\Gamma+\frac{\Gamma_T}{\sigma_{T,c}}\big)\frac{\partial\widetilde{c}}{\partial x_j}\Big]+\langle\rho\rangle\widetilde{S}_c \quad . \tag{2.9}$$

The chemical source term corresponds to a premixed laminar flamelet model, e.g., El Tahry (1990):

$$\langle\rho\rangle\widetilde{S}_c=\rho_u\widetilde{\gamma}/\tau_l \quad , \tag{2.10}$$

where ρ_u is the local unburned gas density, τ_l is a laminar-flame characteristic time, and $\widetilde{\gamma}$ is the probability of being in an active reaction front. In general, a modeled transport equation is solved for $\widetilde{\gamma}$ (El Tahry 1990); here $\widetilde{\gamma}$ is specified algebraically and is proportional to $\widetilde{c}(1-\widetilde{c})$. Local unburned-gas properties are needed to determine ρ_u and τ_l; it is important to recognize that these are not available from $\widetilde{c}$ and $\widetilde{\gamma}$ alone in a moment formulation. In the present formulation, $\rho_u=\langle\rho|c=0\rangle$, the local mean density conditioned on being in the unburned gas.

Equations of state and fluid properties remain the same as for Models 1 and 2. The chemistry is generalized to allow for arbitrary finite-rate chemistry ahead of (Stage I) and behind (Stage III) the primary flame. A composition PDF for the reaction progress variable c and an arbitrary set of species mass fractions is considered; the latter are passive with respect to the thermochemistry. The value of the particle progress variable is either zero (pre-flame) or one (post-flame); the rate of conversion from $c=0$ to $c=1$ is governed by the finite-volume-computed mean (Eq. 2.9). A conventional turbulent mixing model is used (the same pair-exchange model as for Models 1 and 2), but with conditioning on the value of the particle progress variable: pre-flame and post-flame particles cannot mix with one another. The chemical source term also is conditioned on the value of c to allow for different Stage I versus Stage III chemistry:

$$\underline{Y}^{(i)}(t+\Delta t)=\underline{Y}^{(i)}(t)+\underline{S}^{(i)}\big(\underline{Y}^{(i)}(t),c^{(i)}(t),p_0(t)\big)\Delta t+\Delta\underline{Y}_{mix}\big|^{(i)}_{c^{(i)}} \quad . \tag{2.11}$$

Principal finite-volume equations are Eqs. (2.1), (2.2), and (2.9), (2.10) plus equations for $\widetilde{k}$ and $\widetilde{\epsilon}$. Particle positions and compositions evolve by Eqs. (2.3)-(2.5) and (2.11). Mean velocity, mean progress variable, $\widetilde{k}$ and $\widetilde{\epsilon}$ are passed from the finite-volume side to particles; $\langle\rho\rangle$, $\widetilde{\underline{Y}}$, and the unburned-gas properties required for the flamelet model are passed back.

2.3.4. *Model 4*

Model 4 extends Model 3 to multicomponent reacting ideal-gas mixtures and a library-based premixed laminar flamelet model. This is the form that is intended for use in engineering applications (piston engines, in particular). No Model 4 results are presented in this initial report. A skeletal description is provided to indicate salient model features and issues.

The flamelet model adopted is that developed in El Tahry (1990) and Khalighi *et al.* (1995); this includes a modeled equation for $\widetilde{\gamma}$ in addition to Eq. (2.9) for $\widetilde{c}$. A library of one-dimensional steady unstrained premixed laminar flames with detailed hydrocarbon-air chemistry is parameterized in terms of pressure, unburned-gas temperature, equivalence ratio (or mixture fraction), and dilution (Blint & Tsai 1998). A particle enthalpy equation is carried to account for enthalpy (or temperature) fluctuations. Because a mean enthalpy equation is carried on the finite-volume side, consistency between the two representations must be maintained (Muradoglu *et al.* 1999). Particle species mass fractions are no longer passive with respect to thermochemistry. A binary particle progress variable is carried as in Model 3. And as in Model 3, the particle progress variable is used to compute local unburned-gas properties and to switch between Stage I and Stage III chemistry. "Jump conditions" from the flamelet library are used to increment particle compositions as $c^{(i)}$ switches from zero to one. For example, flame-front-generated NO (thermal and prompt) from the flamelet library provides the appropriate initial condition for post-flame thermal NO kinetics corresponding to local thermochemical conditions.

3. Results

3.1. *1D premixed flame propagation in a constant-volume chamber*

This configuration has been selected for its relevance to the piston engine and as a natural extension of the freely propagating turbulent premixed flames that have been studied extensively in the literature. The initial flow is quiescent in the mean. Initial turbulence parameters are the turbulence kinetic energy k_0 and turbulence length scale l_0. The initial rms turbulence velocity, turbulence time scale, and dissipation rate then are given by $u_0' = (2k_0/3)^{1/2}$, $\tau_0 = l_0/u_0'$, and $\epsilon_0 = k_0/\tau_0 = (2/3)^{1/2}k_0^{3/2}/l_0$. The turbulence can be forced so that $\widetilde{k}$ does not decay in the unburned gas, and the turbulence time scale τ can be constrained to remain equal to τ_0 at all times, effectively replacing the dissipation equation. These definitions and constraints facilitate comparison with Anand & Pope (1987). The computational domain has planes of symmetry at $x = 0$ and $x = L$. The flame is ignited at $x = L$ and propagates towards $x = 0$. As the flame propagates, chamber pressure increases; the Mach number is low so that spatial gradients in pressure remain small.

Computations have been performed for a range of aerothermochemical conditions (p_0, T_0, β, k_0, l_0; forcing versus no forcing of turbulence; constant $\tau = \tau_0$ versus standard $\widetilde{\epsilon}$ equation), for different physical models (Model 1, Model 2, Model 3), and for variations in numerical parameters (number of finite-volume cells N_C; number of computational particles N_P). The results presented here correspond to an initial chamber pressure and temperature of $p_0 = 100$ kPa and $T_0 = 300$ K, respectively. The working fluid is an ideal gas having a molecular weight of 24.945 kg/kmol ($\rho_0 = 1$ kg/m^3 at p_0, T_0). The computational domain has a length of $L = 40l_0$. Turbulence is forced and $\tau = \tau_0 =$ constant. A velocity-composition PDF is used (Model 2) with $N_C = 200$, $N_P/N_C \approx 100-200$. For comparison, in a stoichiometric homogeneous-charge automotive

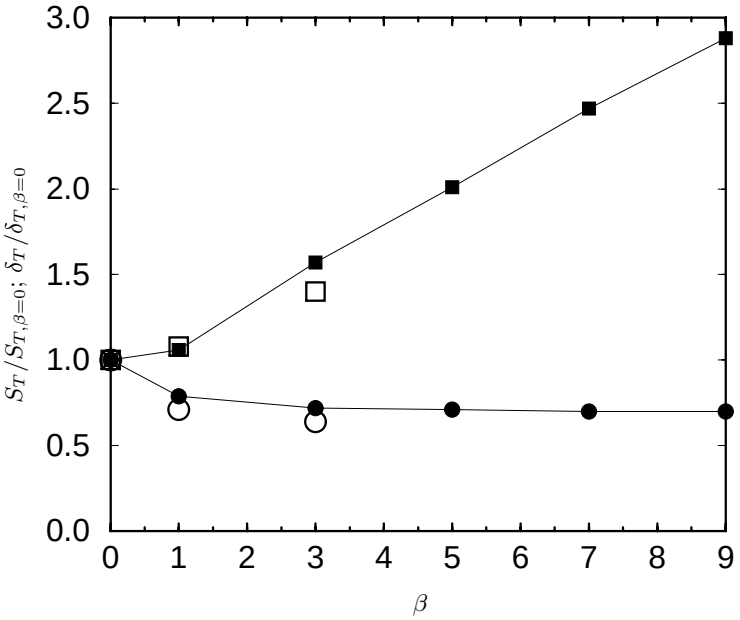

FIGURE 2. Variation of normalized turbulent burning velocity and flame thickness with heat-release for one-dimensional premixed turbulent flame propagation. Open symbols are Model 2 results: ○ $S_T/S_{T,\beta=0}$; □ $\delta_T/\delta_{T,\beta=0}$. Filled symbols are Anand & Pope (1987) results: • $S_T/S_{T,\beta=0}$; ■ $\delta_T/\delta_{T,\beta=0}$.

spark-ignition piston engine at the time of ignition: the clearance height corresponds to 4-8 turbulence integral scales and the bore diameter to 40-80; the pressure and temperature are approximately 15-20 atm and 700-900 K; the heat release parameter is between $\beta = 5$ and $\beta = 6$ with $T_{ref} = 300$ K; and the ratio of unburned- to burned-gas density is between three and four.

With forced turbulence, flame thickness and propagation speed remain approximately constant away from the end planes ($L/4 < x < 3L/4$, say). For $\beta = 0$, the present results are essentially the same as the $R = 1$ results of Anand & Pope (1987). (The density ratio R used there corresponds to the initial unburned- to burned-gas density ratio for the confined flame with $T_{ref} = T_0$; the density ratio decreases in time for the confined flame.) The quasi-steady mass burning rate (or turbulent flame speed S_T) and turbulent flame thickness δ_T, each normalized by their $\beta = 0$ value, are plotted as functions of β in Fig. 2. Here δ_T is the width of the $\widetilde{c} \cdot (1 - \widetilde{c})$ profile. Anand & Pope (1987) results are shown for comparison, using $R = R_0 = \beta + 1$. Global trends are consistent with the freely propagating flame results. The mass burn rate initially drops with increasing β and asymptotes to a value that is about 70% of the $\beta = 0$ value. Flame thickness increases with increasing β; the increase is slow initially and becomes approximately linear with β for $\beta > 1$.

The internal structure of the flame at an instant when it has propagated across approximately one-half of the chamber is shown in Fig. 3 ($\beta = 3$). The mean velocity is zero at $x = 0$ and $x = L$; there is expansion ($\partial\widetilde{u}/\partial x > 0$) through the flame while the gases ahead of and behind the flame are compressed ($\partial\widetilde{u}/\partial x < 0$). A consequence of this

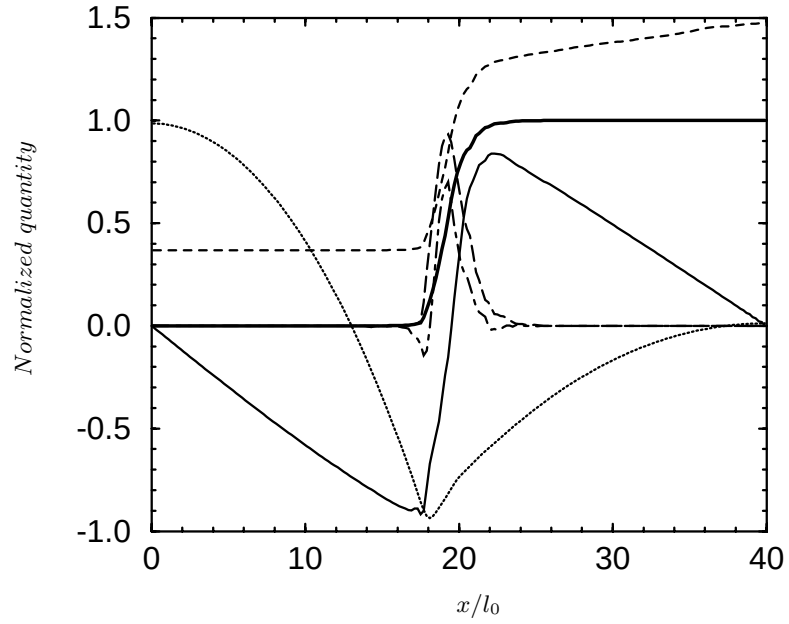

FIGURE 3. Turbulent flame structure at time $t/\tau_0 = 4.62$ for one-dimensional premixed flame propagation in a constant-volume chamber (Model 2, $\beta = 3$): ——— $\widetilde{c}$; ——— $\widetilde{u}/u_0'$; ····· $p'/(100\rho_{u,0}k_0)$; - - - - $T/1000$ K; — — — — $\widetilde{c''^2}$; — — — $\widetilde{u''c''}/u_0'$.

compression is the positive temperature gradient ($\partial T/\partial x > 0$) behind the flame, which results from compressional heating terms in the enthalpy equation (Eq. 2.2).

An important difference between the confined flame and a freely propagating flame is the mean pressure gradient $\partial\langle p\rangle/\partial x$. In Fig. 3, $p'(x) = \langle p(x)\rangle - L^{-1}\int_0^L \langle p(x)\rangle dx$ is the difference between the local mean pressure and the volume-mean chamber pressure. In a steady freely propagating flame, the mean momentum equation reduces to an expression relating the gradient in $\langle p\rangle$ to gradients in $\widetilde{u''^2}$ and $\widetilde{c}$ (Eq. 17 of Anand & Pope 1987); this simplification cannot be made for the unsteady confined flame. The pressure gradient can have a significant influence on flame structure. In particular, $\partial\langle p\rangle/\partial x < 0$ results in preferential $+x$ acceleration of lower-density products ($c = 1$) compared to higher-density reactants ($c = 0$). For sufficiently high density ratio and $|\partial\langle p\rangle/\partial x|$, there is countergradient diffusion in the mean: $\widetilde{u''c''}$ becomes positive, corresponding to a turbulent flux up the gradient in $\widetilde{c}$. Countergradient diffusion is evident through much of the flame thickness at the instant plotted in Fig. 3. However, $\widetilde{u''c''}$ varies considerably in response to changes in the pressure profile as the flame advances.

3.2. *A simple reciprocating-piston engine*

As an initial demonstration for a three-dimensional time-dependent configuration, Model 3 (a composition PDF) is applied to a simple piston engine. Fluid property specification is the same as for the one-dimensional flame-propagation example, and $\beta = 6$ at $T_{ref} =$ 300 K. A coarse mesh of 7,695 volume elements represents a pancake (flat head and piston) combustion chamber having 0.5 L displacement volume (86 mm bore × 86 mm stroke) and a geometric compression ratio of 10:1. Nominal particle number density is

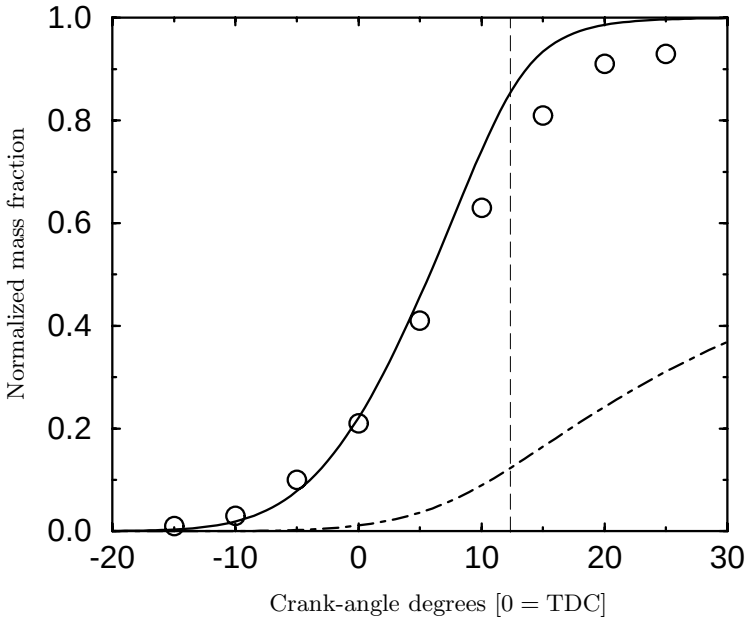

FIGURE 4. Mass-burned fraction and global species 3 mass fraction versus crank angle degrees of rotation for a simple pancake-chamber engine, Model 3: ——— computed mass-burned fraction; — — — computed $10^4 \cdot Y_{3,global}$; ∘ measured mass-burned-fraction curve (typical); - - - - computed location of peak pressure.

25 per cell. Computations are initialized at piston bottom-dead-center; initial pressure and temperature are 100 kPa and 300 K, respectively. The initial mean velocity field has a swirl ratio of 2.0 (angular momentum about the cylinder axis, divided by the fluid moment of inertia about that axis and normalized by the crankshaft rotational speed) and a tumble ratio of 1.0 (similarly normalized angular momentum about an axis normal to the cylinder axis). The initial turbulence kinetic energy is two times the mean piston speed, and the initial turbulence integral length scale is 10 mm. Engine speed is 1200 r/min with ignition at 25 crank-angle degrees before piston top-dead-center. All walls (head, liner, and piston) are isothermal at 600 K.

Three species are carried in addition to the reaction progress variable c. Species 1 and 2 correspond to two trace contaminants that initially are segregated in the axial (z) direction: ($Y_1 = 1$, $Y_2 = 0$ for $z < (z_{piston} + z_{head})/2$; $Y_1 = 0$, $Y_2 = 1$ for $z \geq (z_{piston}+z_{head})/2$). The third species is the product of chemical reaction between species 1 and 2. An irreversible finite-rate Arrhenius reaction of the form $S_3 = AY_1Y_2\exp\{-T/T_a\}$ ($S_1 = S_2 = -S_3/2$) is used with $A = 1$ s^{-1} and $T_a = 10,000$ K. This reaction occurs only after species 1 and 2 have mixed to the molecular level; moreover, because of the high activation temperature, the reaction rate becomes significant only after the primary flame has passed. Species 3 represents a generic trace pollutant.

Computed mass-burned fraction through the combustion event is plotted in Fig. 4. Burn duration corresponds to 50-60 crank-angle degrees of rotation, and the computed location of peak pressure is 12.5° after top-dead-center: there are reasonable values. A typical measured mass-burned fraction curve for an open-chamber engine under similar

operating conditions is shown for reference. Experimental curves typically asymptote to less than 100% total mass burned because of blowby past piston rings and other effects not present in the model. This figure shows that the global rate of heat release (governed by Eulerian flamelet equations, with local unburned-gas properties taken from the particles) is captured reasonably well. The final curve on Fig. 4 shows the computed global mass fraction of pollutant species 3.

4. Concluding remarks

Hybrid PDF/premixed laminar flamelet models and a hybrid Lagrangian/ Eulerian solution methodology have been formulated, implemented, and demonstrated. These provide a framework for incorporating detailed chemical kinetics, realistic turbulence/chemistry interaction, and mixed-mode combustion (Fig. 1) in three-dimensional time-dependent CFD for device-scale applications. The philosophy has been to use the model that most naturally represents the physics at each stage of the combustion process. The principal issue is integration of the different models in a consistent and natural way. While the development has been carried out with spark-ignition piston engines in mind, model formulation and numerical methodology, and to a lesser extent the specific physical models adopted, are intended to be broadly applicable to other mixed-mode combustion systems. Moreover, the approach is readily extended to subgrid-scale combustion modeling for LES using a filtered-density-function method (e.g., Colucci *et al.* 1998); the key difference is in the specification of appropriate turbulence scales.

Subsequent reports will expand on the preliminary findings reported here. This will include: a deeper discussion of confined propagating turbulent premixed flames and differences with respect to freely propagating flames; presentation of parametric numerical studies; and further results for stratified combustion in piston engines.

Acknowledgments

The author thanks the GM Research & Development Center for supporting this project and for providing computer resources. He also thanks the CTR organizers, hosts, and fellow visiting researchers for a stimulating and productive environment in which to carry out this research; in particular, CTR Director Professor Parviz Moin and CTR project host Dr. Heinz Pitsch.

REFERENCES

Anand, M. S. & Pope, S. B. 1987 Calculations of premixed turbulent flames by PDF methods. *Combust. Flame.* **67**, 127-142.

Blint, R. J. & Tsai, P.-H. 1998 C_3H_8-air-N_2 laminar flames calculated for stratified IC engine conditions. *Twenty-Seventh Symposium (International) on Combustion*, The Combustion Institute, Pittsburgh, PA. Poster W1E18.

Colucci, P. J., Jaberi, F. A., Givi, P., & Pope, S. B. 1998 Filtered density function for large eddy simulation of turbulent reacting flows. *Phys. Fluids.* **10**, 499-515.

El Tahry, S. H. 1990 A turbulent combustion model for homogeneous charge engines. *Combust. Flame.* **79**, 122-140.

Haworth, D. C. & Pope, S. B. 1987 A pdf modeling study of self-similar turbulent free shear flows. *Phys. Fluids.* **30**, 1026-1044.

Khalighi, B., El Tahry, S. H., Haworth, D. C., & Huebler, M. S. 1995 Computation and measurement of flow and combustion in a four-valve engine with intake variations. *SAE Paper No. 950287*.

Muradoglu, M., Jenny, P., Pope, S. B., & Caughey, D. A. 1999 A consistent hybrid finite volume/particle method for the pdf equations of turbulent reactive flows. *J. Comput. Phys.* **154**, 342-371.

Peters, N. 2000 *Turbulent Combustion*. Cambridge University Press.

Pope, S. B. 1985 Pdf methods for turbulent reactive flows. *Prog. Energy Combust. Sci.* **11**, 119-192.

Subramaniam, S. & Haworth, D. C. 2000 A pdf method for turbulent mixing and combustion on three-dimensional unstructured deforming meshes. *Int'l. J. Engine Res.* to appear.

Zhao, F., Lai M.-C., & Harrington, D. L. 1999 Automotive spark-ignited direct-injection gasoline engines. *Prog. Energy Combust. Sci.* **25**, 437-562.